Available online at www.sciencedirect.com
ScienceDirect
Journal of Power Sources 179 (2008) 381–387
JOURNAL OF POWER SOURCES
www.elsevier.com/locate/jpowsour

Study of zinc electrodes for single flow zinc/nickel battery application

Li Zhang [a,b,*], Jie Cheng [a,b,*], Yu-sheng Yang [a,b], Yue-hua Wen [b], Xin-dong Wang [a], Gao-ping Cao [b]

[a] *Metallurgical and Ecological Engineering School, University of Science and Technology Beijing, Beijing 100083, China*
[b] *Research Institute of Chemical Defence, Beijing 100083, China*

Received 17 September 2007; received in revised form 20 December 2007; accepted 21 December 2007
Available online 4 January 2008

Abstract

Zinc deposition from alkaline zincate solution in single flow zinc/nickel battery has been investigated. The effect of different substrates such as copper, cadmium and lead were examined by using cyclic voltammetry and cathodic polarization technique. It was found that the cadmium substrate is better than the others. Zinc deposition was carried out by using galvanostatic technique, and the deposits were examined by SEM. The results demonstrated that there is no zinc dendrite on the cadmium substrate in flowing electrolyte. Coulombic and voltage efficiencies of 98 and 88%, respectively, are obtained in a small laboratory cell.

Keywords: Zinc deposition; Single flow zinc/nickel battery; Cadmium substrate; Dendrite

1. Introduction

Redox flow batteries (RFB) characterized by high charge/discharge efficiencies can transform unstable power output into a continuous, safe and reliable output. Such batteries provide an alternative solution to large-scale energy storage technologies for scaling utilization of renewable energy such as solar and wind energy, etc. They are also suited for load leveling/peak shaving, having the potential to increase the flexibility of the power systems and improve the response to a sudden demand of energy.

In the development of redox flow batteries, several RFB systems including Fe/Cr [1], V [2], Zn/Br_2 [3], and polysulfide/Br_2 [4] have been successively proposed and developed. Performance of the batteries has been improved step by step within the past years. However, all the systems require the employment of cells with ion exchange membranes. Such membranes are expensive, not only increase the cost of the battery, but also introduce the complexity and another issues associated with unwanted transport processes through the membranes. A novel redox flow battery system, lead-acid battery system [5–8], which use single electrolyte, was proposed by professor Pletcher in 2004. There is no requirement of ion exchange membranes in this system and the construction of the stack is simple.

Combining conventional zinc–nickel battery with the single flow lead-acid battery, another single electrolyte system, a single flow Zn–Ni battery system, has been proposed by our team [9]. In this battery, $Ni(OH)_2$ is changed to NiOOH at positive and the zincate is reduced to zinc on the negative electrode substrate when charging. The reverse process occurs when discharging.

In conventional Zn–Ni batteries, the collector substrates have little effects on the electrochemical reactions of negative electrodes during charge–discharge due to the excessive zinc active materials. Comparatively, in the case of single flow zinc–nickel batteries, the zinc should be deposited on an inert substrate and dissolved into the solution, alternately. As a result, the nature of the substrate has great effect on the reaction process and the deposition morphology of the zinc.

Effects of the substrates on zinc deposition from zincates solution have been studied [10,11] in low concentration of zinc

* Corresponding authors. Tel.: +86 10 66705840; fax: +86 10 66748541.
E-mail addresses: zhlustb@sina.com (L. Zhang), chengjie_chj@sohu.com (J. Cheng).

0378-7753/$ – see front matter © 2008 Elsevier B.V. All rights reserved.
doi:10.1016/j.jpowsour.2007.12.088

oxide dissolved KOH solution. But, in the single flow Zn/Ni battery, the electrolyte has high concentration of alkaline zincate solution and the quantity of zinc deposit was massive [9], so the substrates may have different effects. Therefore, in the present work, different metal substrates for zinc deposition and the deposition morphology of zinc reduced from high concentration of alkaline zincate solution were studied, and the charge–discharge performance of the cell has also been shown.

2. Experimental

2.1. Pre-treatment of the electrode

The working electrodes used in the stationary electrolytes were prepared as follows. The Copper electrode was cylindrical electrode (purity 99.99%) and embedded in epoxy resin with an exposed cross-sectional area of 0.196 cm^2. After grinding successively with 400#, 800#, 1000# sand papers, the electrodes were cleaned with acetone and then washed by ultrasonic cleaning in deionized water for 15 min prior to measurements. The lead and cadmium electrodes were obtained by electrodepositing on the surface of newly treated copper electrodes as described in Ref. [12]: the cadmium was electroplated for 15 min and the lead was electroplated for 20 min at the same current density of 20 mA cm^{-2}, respectively.

The working electrodes used in flowing electrolytes were cadmium-plated nickel sheet with an electrode area of 10 mm × 10 mm and the cadmium was electroplated at the current density of 20 mA cm^{-2} for 15 min [12].

2.2. Experimental apparatus and procedures

Effect of different electrode substrates on zinc deposition–dissolution was investigated by cyclic voltammetry (CV) and cathode polarization technique.

The CV experiments were conducted in 1 M ZnO + 10 M KOH stationary solution at room temperature in a three-electrode configuration consisting of the sintered nickel hydroxide electrode as the counter electrode and Hg/HgO as the reference electrode. Reagents of analytical grade purity were used, and the electrolyte was prepared with deionized water. The solutions were deaerated by bubbling high purity nitrogen through the solution for 15 min prior to the measurements. All the cyclic voltammogram studies were made in voltage envelopes that were lower than the potential region where the substrate could be oxidized, and the scan rate was 10 mV s^{-1}.

Zinc deposition in stationary electrolyte and flowing electrolyte was conducted at different current density limited by constant charge capacity of 6 C cm^{-2}.

In the case of flowing electrolyte, the experiments were performed at room temperature in a three-electrode configuration as shown in Fig. 1, consisting of a sintered nickel hydroxide electrode with the geometric areas of 10 mm × 70 mm as the counter electrode and Hg/HgO as the reference electrode. After deposition, the electrode was immediately removed from the electrolyte, washed repeatedly in distilled water, rinsed in methanol, and stored in an argon-purged container to prevent additional oxidation of the electrode surface until mounted in the scanning electron microscope (Cambridge S-360).

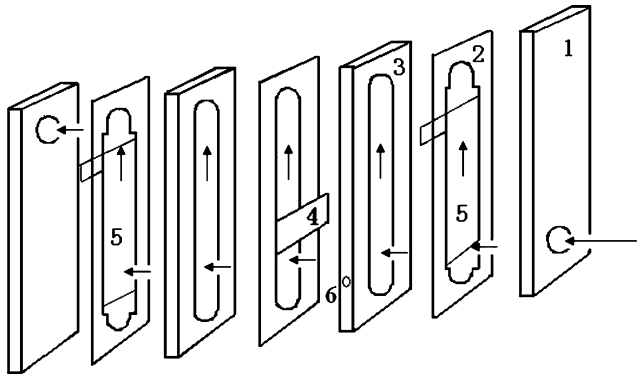

Fig. 1. Schematic diagram of the experimental device for zinc deposition in flowing electrolytes. (1) Perspex end plate; (2) rubber gasket; (3) flow passage: thickness 5 mm; (4) work electrode: 10 mm × 10 mm cadmium-plated nickel plate; (5) counter electrode: 10 mm × 70 mm sintered nickel electrode; (6) location hole of the reference electrode. The flow rate of electrolyte is 19.5 cm s^{-1}.

Finally, the charge/discharge experiments were carried out in a two-electrode cell using a Wuhan Land CT2001A battery test system. A sintered nickel hydroxide electrode was employed as the positive electrode. The areas of positive and negative electrodes were 70 mm × 70 mm.

In this paper, all the experiments were carried out using a computer-controlled Solartron 1280z workstation.

3. Results and discussion

3.1. Cyclic voltammograms

Fig. 2 shows the CV curves on a Cu substrate in the voltage envelopes −0.6 V to the potential ranged from −1.00 to −1.60 V in 1 M ZnO + 10 M KOH. On the curves, there is a well-defined reduced peak at −1.07 V on the cathode scan and two oxidation peaks at about −0.86 and −1.05 V on the anode scan in the voltage envelope −1.00 to −1.15 V as shown in Fig. 2a, indicating a monolayer of underpotential deposited zinc approximately formed on Cu. This is due to the fact that the work function for Cu is much closed to Zn, resulting in the monolayer formed at the potential positive to the Nernst potential prior to bulk deposition. On the monolayer, the crystal nucleus of bulk deposition would be generated, thus this zinc monolayer would influence the growth of deposition layers. It is indicated by researchers [13] that the monolayer of underpotential deposited is uniformly distributed on the surface of substrates rather than only on some active sites, which facilitates the formation of uniform bulk deposition.

As shown in Fig. 2b, with the voltage envelope extended to −1.35 V, no change is observed on the three peaks and there is a shoulder on the cathode scan between −1.1 and −1.35 V. This cathode current shoulder can be ascribed to Cu–Zn alloy formation in the potential region between the Nernst potential and the underpotential deposition region [10]. The two oxidation peaks at about −0.86 and −1.05 V are attributed to the dissolution of the underpotential deposited zinc and the alloy, respectively.

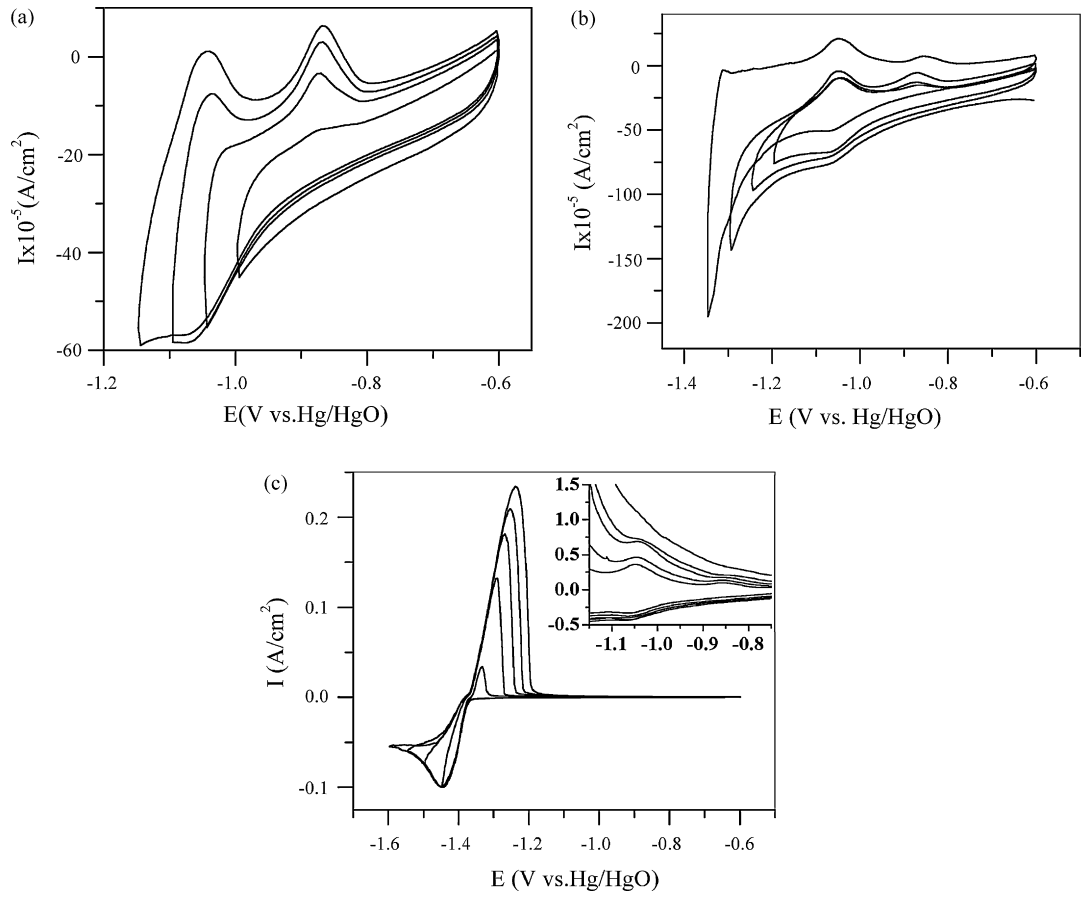

Fig. 2. Cyclic voltammetric curve for potassium zincates solution at copper electrode: (a) −0.60 to −1.15 V; (b) −0.60 to −1.35 V; (c) −0.60 to −1.60 V; sweep rate 10 mV s^{-1}. Hg/HgO as the reference electrode.

When the negative limit is extended from −1.40 to −1.50 V as shown in Fig. 2c, there appears a new cathode peak at about −1.45 V indicating the occurrence of the zinc bulk deposition and the third oxidation peak at about −1.32 V indicating the dissolution of the bulk zinc. This anode peak current increases and shifts to more positive potentials as the end potential extends to more negative. As the cathode scan is extended to −1.60 V, the three anodic current peaks at about −1.32, −1.05 and −0.86 V have no change indicating the reversibility of the reaction in the potential envelope.

From the above data, it can be concluded that there is no discernible nucleation overpotential for zinc deposition on Cu, but the deposition and dissolution of zinc on Cu is fairly a complex process which includes the underpotential deposition/dissolution of zinc and the growth/dissolution of alloy phase and bulk zinc. This is mainly attributed to the alloy formation of zinc with Cu corresponding to the cathodic process at potentials between the underpotential deposition region and the Nernst potential region.

Fig. 3 shows the CV curves on Pb electrode in 1 M ZnO + 10 M KOH in different potential envelopes. It can be seen that the deposition and dissolution processes of zinc on Pb is different from those on Cu. No underpotential deposition of zinc is observed. At −1.45 V there is a cathode current peak of zinc bulk deposition and the corresponding anodic current

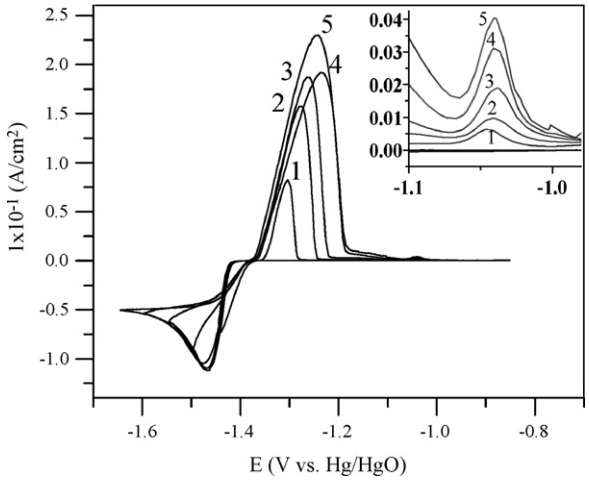

Fig. 3. Cyclic voltammetric curve of lead electrode in potassium zincates solution: (1) −0.60 to −1.45 V; (2) −0.60 to −1.50 V; (3) −0.60 to −1.55 V; (4) −0.60 to −1.60 V; (5) −0.60 to −1.65 V; sweep rate 10 mV s^{-1}. Hg/HgO as the reference electrode.

peak at −1.32 V is the dissolution of bulk zinc. There is only one cathode peak observed, this is different from that described in literature [11].

The inset in Fig. 3 shows a small anodic peak appearing at −1.05 V similar to that in Fig. 2, this anodic peak can be

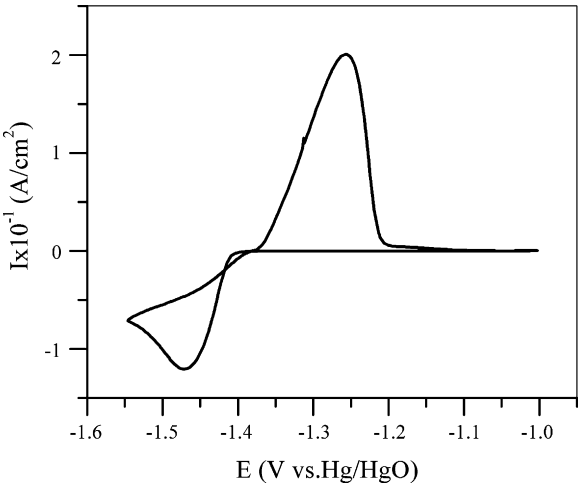

Fig. 4. Cyclic voltammetric curve of cadmium electrode in 1 M ZnO + 10 M KOH solution; sweep rate 10 mV s^{-1}. Hg/HgO as the reference electrode.

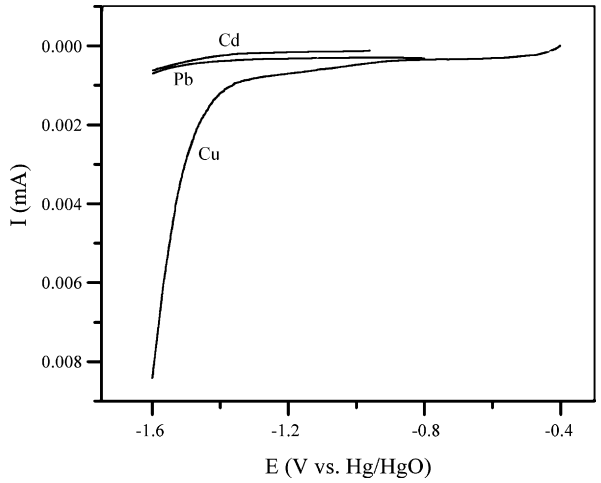

Fig. 5. Cathode polarization curves of copper, lead and cadmium electrode in 10 M KOH.

assigned to the dissolution of zinc in the Cu–Zn alloy. It is known that the diffusivity of Zn in Pb is abnormally high, namely, 8.24×10^{-11} cm^2 s^{-1} at 25 °C [14]. It is about six orders of magnitude higher than the self-diffusion of Pb in Pb. But no Pb–Zn alloy can be formed. Accordingly, zinc passes through the deposited Pb layer followed by alloy formation with Cu in the process of zinc deposition.

Fig. 4 is a CV curve on Cd in 1 M ZnO + 10 M KOH in the voltage envelope −1.00 to −1.55 V. It can be observed that the deposition/dissolution of zinc on Cd is rather simpler than that on Cu or Pb. There is no evidence of underpotential deposition or alloy formation. It is maybe due to the fact that zinc cannot pass through the deposited Cd layer. The current peak can be attributed simply to bulk zinc deposition at −1.45 V and dissolution at −1.25 V.

In the process of zinc deposition, hydrogen evolution is a main parasitic reaction. So the behavior of hydrogen evolution on electrodes is an important factor which influences the deposition of zinc. Fig. 5 presents the cathodic polarization curves for the Cd, Pb and Cu substrates in 10 M KOH solution. It is found that the overpotential of hydrogen evolution on Cd is higher than that on Pb or Cu, and then there will be the highest efficiency of zinc deposition on Cd.

From the above investigations, it is confirmed that the deposition/dissolution process of zinc on Cd is rather simple, benefiting the discharge of zinc. In addition, the efficiency of zinc deposition on Cd is higher due to the high overpotential of hydrogen evolution on Cd. Therefore, Cd should be an excellent substrate for the deposition of zinc. It was pointed out by Oswin and Blurton [15] that no matter the zinc deposition was controlled by diffusion or by activation, the weight of adherent deposit for the same amount of zinc deposited on different substrates varied with the substrate according to Cd > Ag, Zn > Cu. This also indicates that the adhesion of zinc deposits on Cd is preferable. Thus, cadmium-plated current collectors have been selected to be used in single flow zinc/nickel battery, and only the results on cadmium electrodes were presented in the following experimental.

3.2. Deposit morphology of zinc

To understand more clearly the effect of flowing electrolytes on the deposition of zinc, the characteristic patterns of electroplating process and the deposit morphology of zinc in stationary electrolytes and flowing electrolytes were studied, respectively, for comparison. The curves of deposition potentials vs. time at different current densities are shown in Fig. 6. In the case of stationary electrolytes as shown in Fig. 6a, the deposition potentials of zinc become more negative with the increase of the

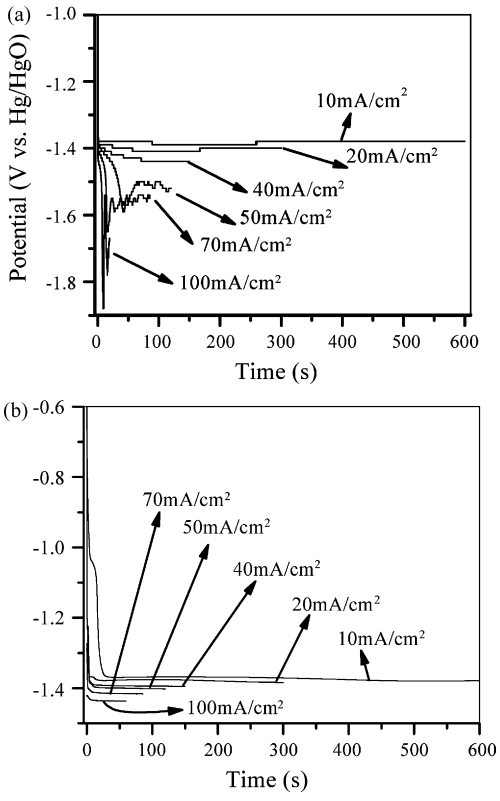

Fig. 6. Potential–current density curve for Cd electrode in 1 M ZnO + 10 M KOH solution: (a) stationary electrolyte; (b) flowing electrolyte.

current density, and, there is a phenomenon of potential oscillating on first starting of the measurements when the current density exceeds 50 mA cm^{-2}. Furthermore, when the current density increases from 50 to 100 mA cm^{-2}, the time when the potential begins to oscillate continues to be shorter with a larger magnitude of oscillation. It is caused by the fact that the zincates ion concentration at the electrode surface is approximately nil when zinc is deposited at a high current density, resulting in the decrease of electrode potential closed to the hydrogen evolution potential and then generated hydrogen. When the electrolyte is stirred by escaping hydrogen gases, the zincates ion concentration at the electrode surface is not nil any more. Accordingly, the potential increases to be closed to the original value. As a result, an oscillating image appears on the curves of initial potential vs. time. With the time prolonged, the growth of a large number of thin zinc polyhedral platelets or dendrites crystal causes a large increase in the reaction area for zinc deposition and hence a large decrease in the real current density under the constant current, which leads to a positive shift of the potential at which reaction-limited electrode deposition proceeds, and the diffusion limited condition for Zn^{2+} is largely reduced, then the potential keep almost invariableness.

In the case of flowing electrolytes, as shown in Fig. 6b, the potentials for zinc deposition basically remains unchanged at different current densities, and the potential decreases from −1.37 to −1.43 V with a change of 60 mV as the current density increasing from 10 to 100 mA cm^{-2}. Also, there is no potential oscillation resulting from hydrogen evolution. It is mainly attributed to the fact that the flowing electrolyte can effectively enhance the mass transportation of zincates ions,

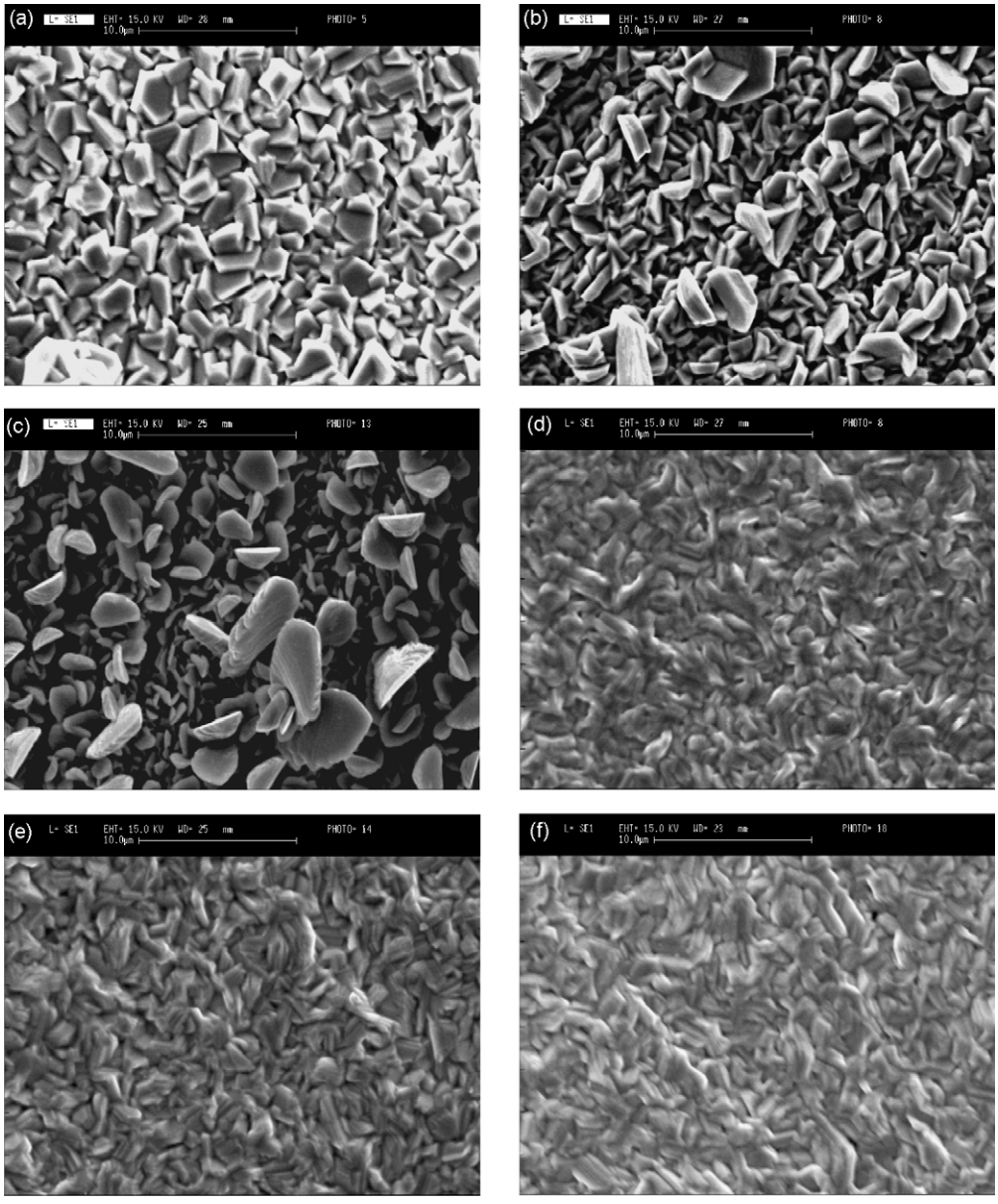

Fig. 7. Surface morphology of the deposited zinc at different current density in still electrolyte: (a–c) (current density 50, 70, 100 mA cm^{-2}) and fluent electrolyte: (d–f) (current density 50, 70, 100 mA cm^{-2}).

making the electrode process controlled by electrochemical activation.

At the same time, the morphology of zinc deposits was characterized by SEM images as shown in Fig. 7. The change of the morphology of zinc deposited in stationary electrolytes with the current density is given in Fig. 7a–c, respectively. It is known that the dendrite growth is easier to occur at high current densities due to diffusion controlled deposition conditions. So, the current densities for comparative investigation are selected to be 50 mA cm^{-2} (Fig. 7a), 70 mA cm^{-2} (Fig. 7b) and 100 mA cm^{-2} (Fig. 7c). From Fig. 7a, it is observed that the morphology of zinc deposited at 50 mA cm^{-2} displays a structure of hexagonal platelets with about 3 μm in length. The surface of zinc deposits is oriented parallel to the basal plane, and the deposits are distributed evenly and relatively compact. As the current density increases to be 70 mA cm^{-2}, small dendrites with a dimension of around 4 μm start to appear in the zinc deposits as shown in Fig. 7b. The deposits are not dense any more and the deposited particles grow upward. At the current density of 100 mA cm^{-2}, big dendrites are formed with a dimension of up to 6–7 μm.

Scanning electron micrographs of zinc deposits in flowing electrolytes with the same velocity of 19.5 cm s^{-1} were shown in Fig. 7d (50 mA cm^{-2}), 7e (70 mA cm^{-2}) and 7f (100 mA cm^{-2}). The deposition condition is 6 C cm^{-2} at current densities ranged from 50 to 100 mA cm^{-2}. There are great differences between the morphology of zinc deposits in flowing electrolytes and those in stationary electrolytes. With the current density increasing, scarcely any dendrite growth is found in the zinc deposits and, in fact, compact zinc deposits with crystal particles of about 2 μm are formed, which is independent of the current density.

Therefore, zinc dendrites can be inhibited significantly by employing flowing electrolytes with a certain velocity. It will be beneficial for improving the cycling performance of the zinc/nickel battery.

3.3. Battery performance

In order to demonstrate the effect of cadmium-plated electrode and flowing electrolyte on the capacity and cycle life of the single flow zinc/nickel cell, a number of charge/discharge cycle experiments were carried out at the current density of 10 mA cm^{-2} in a two-electrode laboratory cell. The configuration of the cell is similar to Fig. 1, wherein a sintered nickel with an average surface capacity of 25 mAh cm^{-2} was employed as the positive electrode, a cadmium-plated copper plate was employed as the negative electrode substrate, and the electrode area of the two electrodes is 70 mm × 70 mm. A typical charge–discharge curve is given in Fig. 8a. From this plot, the average values of charge and discharge voltage were 1.85 and 1.66 V, respectively. Fig. 8b shows the variation of coulombic efficiency and energy efficiency with cycle number of the cell.

It can be seen that the coulombic and energy efficiencies of the cell basically remain unchanged over 220 cycles, obtaining an average coulombic efficiency of about 98% and an average energy efficiency of about 88%. This indicates that the performance of the single flow zinc/nickel battery experiences no deterioration over 220 charge–discharge cycles; both the cycle performance and energy efficiency are enhanced considerably. Further experiments are being performed.

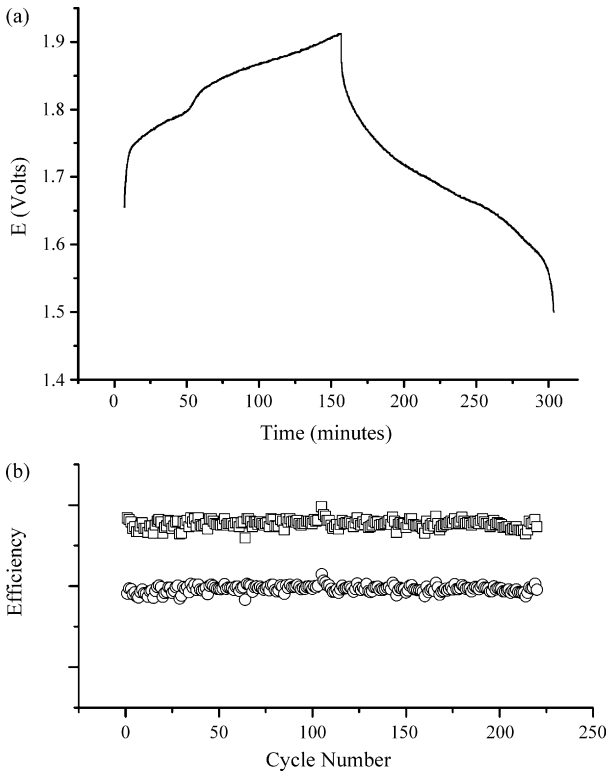

Fig. 8. (a) charge–discharge curve; (b) coulombic efficiency, and energy efficiency during 220 cycles.

4. Conclusions

The deposition and dissolution of zinc on Cu, Pb and Cd substrate from concentrated alkaline zincates solutions have been investigated using cyclic voltammetry, the results show that the electroplating behavior of zinc on Cu and Pb is fairly complex, whereas in the case of Cd the electroplating behavior is simple, facilitating the discharge of zinc.

The deposit morphology of zinc in stationary electrolytes and in flowing electrolytes is characterized by scanning electron microscopy. It is found that small dendrite growth occurs at a current density of above 70 mA cm^{-2} in stationary electrolytes, while in flowing electrolytes scarcely any dendrites are formed at any current densities adopted, obtaining compact zinc deposits with tiny crystal particles.

Preliminary tests were performed using small laboratory cells to evaluate the charge–discharge performance of the single flow zinc/nickel battery. Results showed that average coulombic and energy efficiencies achieved are remained 98 and 88% over 220 cycles, respectively, by employing a cadmium-plated substrate as the negative electrode. This indicated that the preferable battery performance is obtained.

References

[1] M. Shimada, Y. Tsuzuki, Y. Lizuka, M. Inoue, Chem. Ind. 3 (1988) 80.
[2] R.J. Remick, P.G. Pang, US Patent 4,485,154, 1984.
[3] P. Lex, B. Jonshagen, Power Eng. J. 13 (1999) 142.
[4] M. Skyllas-Kazacos, F. Grossmith, J. Electrochem. Soc. 134 (1987) 2950.
[5] A. Hazza, D. Pletcher, R. Wills, Phys. Chem. Chem. Phys. 6 (2004) 1773.
[6] D. Pletcher, R. Wills, Phys. Chem. Chem. Phys. 6 (2004) 1779.
[7] D. Pletcher, R. Wills, J. Power Sources 149 (2005) 96.
[8] A. Hazza, D. Pletcher, R. Wills, J. Power Sources 149 (2005) 103.
[9] L. Zhang, J. Cheng, Y.Sh. Yang, Y.-H. Wen, G.-P. Cao, X.-D. Wang, Electrochem. Commun. 9 (2007) 2639–2642.
[10] M.G. Chu, J. McBreen, G. Adzic, J. Electrochem. Soc. 128 (1981) 2281.
[11] M.G. Chu, J. McBreen, G. Adzic, J. Electrochem. Soc. 128 (1981) 2287.
[12] Y.Ch. Zhang, R.N. Hu, R. Xiang, Electroplating Manual, National Defence Industry Press, 2007 (in Chinese).
[13] M.M. Nicbolson, J. Am. Chem. Soc. 79 (1957) 7.
[14] R.A. Ross, H.B. Vanfleet, D.L. Decker, Phys. Rev. B 9 (1974) 4026.
[15] A. Fleischer, J.J. Lander, Zinc–Silver Oxide Batteries, John Wiley & Sons, New York, 1971, p. 63.